

## Effect of twist, fineness, loading rate and length on tensile behavior of multifilament yarn\*

Rostislav Ryp1, Miroslav Vořechovský<sup>2</sup>, Britta Sköck-Hartmann<sup>3</sup>, Rostislav Chudoba<sup>4</sup>, Thomas Gries<sup>5</sup>

**Summary:** The idea underlying the present study was to apply twisting in order to introduce different levels of transverse pressure. The modified structure affected both the bonding level and the evolution of the damage in the yarn. In order to isolate this effect in a broader context, additional parameters were included in the experiment design, namely effects of loading rate, specimen length and filament diameter (directly linked to the fineness of the yarn). These factors have been studied in various contexts by several authors. Some related studies on involved factors will be briefly reviewed.

### 1 Introduction

Textile fabrics are increasingly applied as a reinforcement of concrete structures in civil engineering realizations [1], [2] and [3]. In this application domain, alkali resistant glass fibers and carbon fibers as well as aramid fibers and high modulus polyethylene fibers are used as reinforcement materials. At present, most emphasis is put on alkali resistant (AR) glass fibers as they are comparatively cheap while having a high tenacity. Therefore, AR-glass yarns have been chosen to perform a detailed study of failure process under varied conditions. The test program was accompanied by the development and utilization of fiber bundle models [4] [5].

When applied as reinforcement, yarns are not fully penetrated by the matrix. A better bond to the matrix develops only in the outer region of the yarn cross section. Inner filaments are bonded only through the filament-filament interaction resulting in much lower bond shear stress compared to the outer bond filament-matrix. However, as documented in [6] the effect

\* This is a peer-reviewed paper. Online available: [urn:nbn:de:bsz:14-ds-1244041881719-95100](https://nbn-resolving.org/urn:nbn:de:bsz:14-ds-1244041881719-95100)

<sup>1</sup> Dipl.-Ing., RWTH Aachen University, Institute of Structural Concrete

<sup>2</sup> Asoc.-Prof. PhD, Faculty of Civil Engineering, Brno University of Technology, Institute of Structural Mechanics

<sup>3</sup> Dipl.-Ing., RWTH Aachen University, Institute for Textile Technology

<sup>4</sup> Dr.-Ing., RWTH Aachen University, Chair of Structural Statics and Dynamics

<sup>5</sup> Univ.-Prof. Dr.-Ing. Dipl.-Wirt. Ing., RWTH Aachen University, Institute for Textile Technology

of the inner bond on the macroscopic performance of a reinforced tensile specimen cannot be neglected. While the outer bond affects the behavior at the length scale of a crack distance, the inner bond influences the failure process at the length scale of a structural element with sufficiently large stress transfer (or anchorage) length. This can be documented by a significant contribution of the inner bond to the stress level in the post-cracking regime of a tensile specimen reinforced with AR-glass yarns.

Since it is impossible to directly test the *in-situ* filament-filament interaction due to the complex packing of filaments in the yarn with a high amount of irregularities, different levels of transverse pressure between filaments in the yarn were performed. This can be obtained by applying a certain twist level. In order to isolate this effect in a broader context, additional parameters have been included in the experiment design, namely effects of loading rate, specimen length and filament diameter (directly linked to the fineness of the yarn).

Fully statistical theory for the strength of twisted bundles has been formulated using the strain-based fiber bundle model [8] by incorporating the fiber helical paths [10]. However, the theory also excludes fiber interactions such as friction between fibers which is, in reality, strongly strengthened by lateral compression in highly twisted yarns. This effect has been theoretically well documented in [11] using a model including fragmentation. The increased inter-filament bond is included using the chain of fiber bundle models of the critical length representing the stress transfer length needed to recover the filament force. Verbal description of the fragmentation process is presented in [12] on a particular example of a surface treatment strongly affecting the yarn performance. A thorough study on the fragmentation process using a stochastic model has been given in [13].

A comprehensive experimental study of twisted continuous glass yarns has been presented by [14]. In this study, no increase of yarn strength due to twist has been observed. As a consequence the data could be well reproduced by the classical interaction-free models presented in [9]. The same holds for tests of Glass/Nylon blended continuous yarns presented later in [17]. The authors reported tenacity and modulus decrease with increasing twist level while gaining greater total elongation-to-break and less “kinky” behavior. On the other hand, a strength increase up to an optimum twist level has been observed in tests on polymeric yarns in [18]. However, this work was primarily focused on improved reflection of the apparent yarn stiffness (effective tensile  $E$ -modulus).

Summarizing, it is unclear from the reviewed literature whether or not the twisting of studied AR-glass yarns can lead to strength increase due to higher bond with associated fragmentation. While it was not reported in [14], it should be, at least in some range of twist levels, observable according to [11] and [13].

In order to clarify this issue experimentally in a general context, a complex testing program has been prepared and analyzed using the methodology of Design of Experiments [15]. The above discussed test parameters have been varied simultaneously and not on the one-at-a-

time basis. This approach allowed us to justify the constructed response surfaces based on their statistical significance.

## 2 Test setup

A tensile testing motion controlled machine Z100 of Zwick Roell Gruppe, Ulm, was used for the experiments. The tensile force is determined with a load cell at the upper clamping and transformed to nominal stress. The nominal stress is used for comparison purposes of apparent yarn performance under various conditions and does not reflect changes at structural level such as the fiber volume fraction. The strain is obtained by dividing the control displacement by the clamp distance. Loading velocity can be varied within the range from 2.5 to 200 mm/min.

Specimen ends were embedded in epoxy resin to prevent slippage and damage of filaments during testing. The preparation of the specimens was performed using rubber molds. The relatively low modulus of epoxy results in a gradual transfer of loading into the filaments preventing their brittle failure in the clamping. It has a Young's modulus of 3.250 GPa, a tensile strength of 63 MPa and a maximum strain of 8.7 %. The length of the blocks is 75 mm, their width and thickness are 8 mm. The ends of the yarns are embedded in separate molds so that the length could be arbitrarily adjusted up to the maximum distance of the jaws of the testing machine (approx. 500 mm).

The introduction of twist is a crucial aspect of the specimen preparation. Both manual and automated twisting has been applied. In the former case, the specimen has been fixed at the upper jaw of the machine and manually twisted at the bottom end and then fixed in the jaw. In the latter case, industrially produced spun yarns delivered on the bobbins were tested. The automated twisting has been performed under light pre-stress stabilizing the production process. The preliminary tests on the industrially twisted yarns indicated high level of initial damage that totally drowned the effect of twist on the overall yarn strength. For this reason, the manual twisting without pre-stressing has been chosen for the present study. In view of this study the technology was not of primary interest, the focus was on the reproducibility of the studied effects. The additional manual effort was negligible.

Visual impression is that the twist level is not uniform over the yarn length, especially in the case of high twist levels. The helix length varied rather strongly in the range 2-10 cm, see Figure 1 top right for illustration. The reason is probably an irregular structure of multifilament yarn including non-uniformity of lengths. This fact should be kept in mind when modeling the yarn response as it would induce scatter of *in-situ* filament-filament interaction along the yarn.

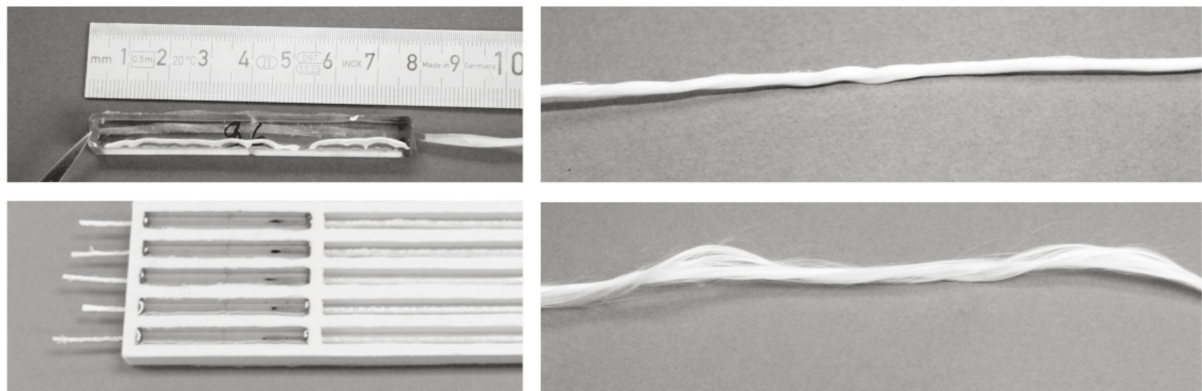


**Fig. 1:** Preparation of the specimens. Left: epoxy-resin blocks and rubber molds for casting. Right: highly twisted specimen before (top) and after (bottom) tensile test.

The tested material was AR-glass yarn (in particular the roving named CemFIL Direktroving LTR 5325 produced by Saint Gobain Vetrotex). The weight fraction of sizing is approximately 0.8 %. The yarn was delivered with three nominal finenesses (640, 1200, 2400 tex).

### 3 Experiment design

The goal of the study is to capture the effect of twist in combination with other possibly interacting effects on the total performance of the bundle. In particular, the multivariate study has been performed with the goal to identify the range of tested parameters with evidently positive effect of transverse pressure on the increased inner bond performance and to make the trends in the response change evident in terms of the statistical design of experiments. The considered interacting factors are the twist level (A), specimen length (B), loading rate (C) and fineness (D).

The chosen levels of the four input factors are given in Table 1. Specified is also the number of runs performed for each combination of levels. In order to reduce the total number of tests the experiment design was constructed in two steps. In the first phase (design I) 200 tests were conducted with all four factors varied at up to four levels (twist) in order to identify/exclude interactions and to construct the initial response surfaces.

Based on these results further 102 tests (design II) were performed within an adjusted design space reduced to two dimensions (twist and fineness). Further, the tested range of twist has been narrowed to the range capturing the maximum effect on the yarn strength with the goal to confirm the shape of the response surface.

**Table 1:** Summary of the experimental design: numbers of realizations for each factor combination. Numbers in parentheses denote experiments belonging to the refined design (II). The six stars denote six censored outliers.

| B:<br>Strain<br>rate<br>[%/min] | D:<br>Fine-<br>ness<br>[tex] | C: Length [mm]     |    |    |    |           |      |        |         | Σ  |    |           |             |
|---------------------------------|------------------------------|--------------------|----|----|----|-----------|------|--------|---------|----|----|-----------|-------------|
|                                 |                              | 250                |    |    |    | 500       |      |        |         |    |    |           |             |
|                                 |                              | A: Twist [turns/m] |    |    |    |           |      |        |         |    |    |           |             |
|                                 |                              | 0                  | 20 | 40 | 60 | 0         | 10   | 20     | 40      | 60 |    |           |             |
| 1                               | 640                          | 2                  | 2* |    | 11 | 8         |      |        | 5       |    |    | 28        | 73          |
|                                 | 1200                         | 7                  |    |    |    | 1         |      |        |         |    | 6  | 14        |             |
|                                 | 2400                         | 6                  |    | 6  | 3  | 6         |      |        | 2       |    | 8  | 31        |             |
| 8                               | 640                          | 7                  |    | 1  |    |           |      |        |         |    | 7  | 15        | 41          |
|                                 | 1200                         |                    |    | 3  |    | 1         |      |        | 5       |    |    | 9         |             |
|                                 | 2400                         | 2                  |    |    | 7* | 6         |      |        |         |    | 2  | 17        |             |
| 40                              | 640                          | 7                  |    | 5  | 4  | 7 (6)     | (10) | (10*)  | (10*)   |    | 10 | 33 (36)   | 86<br>(102) |
|                                 | 1200                         | 1                  | 1  |    | 6  | 6         | (10) | (10)   | 1 (10)  |    |    | 15 (30)   |             |
|                                 | 2400                         | 11                 |    |    | 8* | 6 (6)     | (10) | (10*)  | 6 (10)  |    | 7  | 38 (36)   |             |
| Σ                               |                              | 43                 | 3  | 15 | 39 | 41 (12)   | (30) | 7 (30) | 12 (30) | 40 |    | 200 (102) |             |
|                                 |                              | 100                |    |    |    | 100 (102) |      |        |         |    |    |           |             |

The chosen levels of tested factors (**A-D**) were set based on the following considerations:

**A: Twist** has been introduced manually with one end of the specimen clamped in the upper jaw of the test machine. The lower end was twisted up to the prescribed level [turns/m]. The design included 0, 20, 40, 60 turns/m. An additional twist level of 10 turns/m has been added in the refined design (II).

**B: Loading rate** has been imposed at three levels: 1, 8, 40 %/min. The small rate represents the lower bound of loading rates appearing in structural composite elements. However, it is necessary to include higher rates introduced by the damage process of the composite material, namely by the rate of crack initiation. The applied test set-up allowed us to reliably cover the rate range with upper level set to 40 %/min.

**C: Specimen length** has been tested at two levels (250 and 500 mm) in order to assure that there is no strength reduction due to imperfections of filament fixing at the clamps and due to filament slack. As documented on an example of AR-glass yarn 2400 tex [4] these effects vanish on specimens longer than 100 mm. The second source of strength reduction, namely the statistical size effect in the sense of the weakest-link model was thoroughly tested and described for the tested material in the chosen range of lengths [5]. Based on these studies, the two lengths have been chosen primarily in order to capture interactions of length with the other factors.

**D: Fineness** can be varied only within the levels available commercially. The studied vetrotex yarn was available with 320, 640, 1200, 2400 tex. The 320 tex yarn has not been tested since it differs in the production technology: it is produced by halving the 640 tex yarn. As apparent from Table 2 the variation of fineness induces in fact a variation of filament

diameter since the (approximate) number of filaments  $n = 1600$  is identical for all fineness levels.

Since the chosen number of levels varies for each factor, it was impossible to choose a standard design so that the general *D-optimum* design for constructing the response surfaces by linear regression was used [15]. As the testing has been performed over several days the order of test runs has been randomized with the goal to minimize errors due to uncontrollable factors.

## 4 Results and discussion

### 4.1 Design I

The normalized yarn strength obtained for all the combinations of levels is summarized in Table 2 in terms of the mean and standard deviation. The significance level of the studied effects has been evaluated using the standard procedure of analysis of variance (ANOVA), see e.g. [15], [16]. The evaluation is based on comparing the variance of the data with respect to the model to the variance with respect to a reduced model. In simple terms, we test whether or not the trends proposed by the model could be the result of noise (null hypothesis). If this hypothesis can be rejected at the required significance level the trends are considered to be evident. In our case ANOVA identified all terms of the computed equation as strongly evident except for the factor **C**. Further, the interaction **BC** has been classified as less evident since the ranges of measured values partially overlap. Furthermore, using ANOVA 2 outliers could be detected. Subsequent visual inspection of the specimens confirmed production errors so that these tests were discarded from the design. The obtained response surface contains only the significant effects and interactions. Evaluation of the main effects has shown a nonlinear (cubic) effect of twist (**A**). The effect of loading rate (**B**) was assessed significant for linear term but not for the quadratic one. The obtained rate dependency corresponded with the results presented in [7] for E-glass yarns. As desired, the effect of the specimen length (**C**) turned out to be insignificant, which means that the statistical size effect was negligible in the tested length range. However, its effect had to be retained in the analysis due to the interaction of length with the twist level. The main effect of fineness (**D**) was evaluated as quadratic.

Interactions that turned out to be statistically insignificant are **AB** (twist and loading rate), **CD** (length and fineness), **BD** (loading rate and fineness). The most significant interaction was detected for **AD** (twist and fineness).

**Table 2:** Yarn strength  $\sigma_{\max}$  [MPa] statistics: mean (standard deviation).

| B:<br>Strain rate<br>[%/min] | D:<br>Fine-ness<br>[tex] | C: Length [mm]     |                   |                   |                   |                   |                   |                   |                   | $\Sigma$          |                   |                   |                   |
|------------------------------|--------------------------|--------------------|-------------------|-------------------|-------------------|-------------------|-------------------|-------------------|-------------------|-------------------|-------------------|-------------------|-------------------|
|                              |                          | 250                |                   |                   |                   | 500               |                   |                   |                   |                   |                   |                   |                   |
|                              |                          | A: Twist [turns/m] |                   |                   |                   |                   |                   |                   |                   |                   |                   |                   |                   |
| 0                            | 20                       | 40                 | 60                | 0                 | 10                | 20                | 40                | 60                |                   |                   |                   |                   |                   |
| 1                            | 640                      | 1060.3<br>(28.0)   | 1268.6<br>(0)     |                   | 1094.5<br>(134.4) | 885.8<br>(50.0)   |                   |                   | 1205.8<br>(76.4)  |                   | 1057.2<br>(155.8) | 959.4<br>(207.7)  |                   |
|                              | 1200                     | 1090.9<br>(94.1)   |                   |                   |                   | 1194.6<br>(0)     |                   |                   |                   | 1076.2<br>(31.6)  | 1092.0 (75.6)     |                   |                   |
|                              | 2400                     | 981.2<br>(85.4)    |                   | 848.2<br>(68.7)   | 636.7<br>(26.6)   | 882.8<br>(110.3)  |                   |                   | 1196.8<br>(100.0) |                   | 584.0<br>(65.2)   |                   | 814.5 (198.0)     |
| 8                            | 640                      | 1086.4<br>(42.2)   |                   | 1358.1<br>(0)     |                   |                   |                   |                   |                   |                   | 1269.3<br>(143.5) | 1189.8<br>(142.3) | 1096.6<br>(278.0) |
|                              | 1200                     |                    |                   | 1368.6<br>(127.1) |                   | 1271.9<br>(0)     |                   | 1482.0<br>(115.3) |                   |                   | 1420.9<br>(135.0) | 1420.9<br>(135.0) |                   |
|                              | 2400                     | 1042.5<br>(94.3)   |                   |                   | 690.2<br>(70.0)   | 929.0<br>(79.5)   |                   |                   |                   |                   | 713.4<br>(41.7)   | 826.7 (154.5)     |                   |
| 40                           | 640                      | 1208.8<br>(68.6)   |                   | 1407.8<br>(91.6)  | 1255.7<br>(47.1)  | 1078.3<br>(89.8)  | 1302.0<br>(92.7)  | 1338.9<br>(92.5)  | 1433.8<br>(97.1)  | 1451.2<br>(78.6)  | 1298.9<br>(157.6) | 1242.1<br>(224.6) |                   |
|                              | 1200                     | 1286.9<br>(0)      | 1665.2<br>(0)     |                   | 1168.1<br>(82.2)  | 1240.1<br>(71.7)  | 1470.3<br>(79.4)  | 1579.0<br>(82.3)  | 1488.1<br>(105.6) |                   | 1428.1<br>(170.2) |                   |                   |
|                              | 2400                     | 1070.5<br>(74.9)   |                   |                   | 765.7<br>(72.6)   | 1011.7<br>(75.7)  | 1268.0<br>(71.9)  | 1306.6<br>(114.4) | 1085.4<br>(126.8) | 880.7<br>(79.9)   | 1072.9<br>(185.5) |                   |                   |
| $\Sigma$                     |                          | 1089.7<br>(102.5)  | 1466.9<br>(198.3) | 1172.8<br>(280.0) | 959.0<br>(240.5)  | 1019.3<br>(142.2) | 1346.8<br>(120.4) | 1411.5<br>(159.7) | 1284.6<br>(210.5) | 1052.9<br>(332.0) | 1153.7 (258.4)    |                   |                   |
|                              |                          | 1060.5 (222.1)     |                   |                   |                   | 1199.1 (262.6)    |                   |                   |                   |                   |                   |                   |                   |

Before focusing on the **AD** interaction in detail we have to address a somewhat suspicious result concerning the interaction identified between **BC** (loading rate and length). Here a comparison reveals an inverse length effect for rapid loading (40 %/min). This would suggest a hardly acceptable conclusion saying that the more flaws along the yarn are available (longer specimens) the stronger "healing" effect of the increased loading rate. Even though this trend was assessed as less significant in terms of ANOVA compared to the other listed effects, it cannot be simply clarified and requires further investigation.

It can be concluded that the shape of the response surfaces is similar for all combinations of length and loading rate. Moreover, that the maximum strength is achieved for the combination with the same twist (20 turns/m) and fineness (1200 tex) independently of the loading rate and length. This result suggests that with the present experiment design we were able to isolate a general effect of strength increase for moderate number of turns/m (0-20) with subsequent strength reduction for higher twist levels.

## 4.2 Design I+II

While design I was mainly prepared for a qualitative screening of the studied parameter space, the second design was arranged with the goal to confirm the main effects and interactions with more focused resolution of twist levels: 0, 10, 20 and 40 turns/m (see Table 1). The levels of loading rate and specimen length were fixed to 40 %/min and 500 mm, respectively. This was justified by the low interactions of these factors with the twist and fineness. The analysis of variance detected three outliers that have been censored after visual inspection, see Table 1.

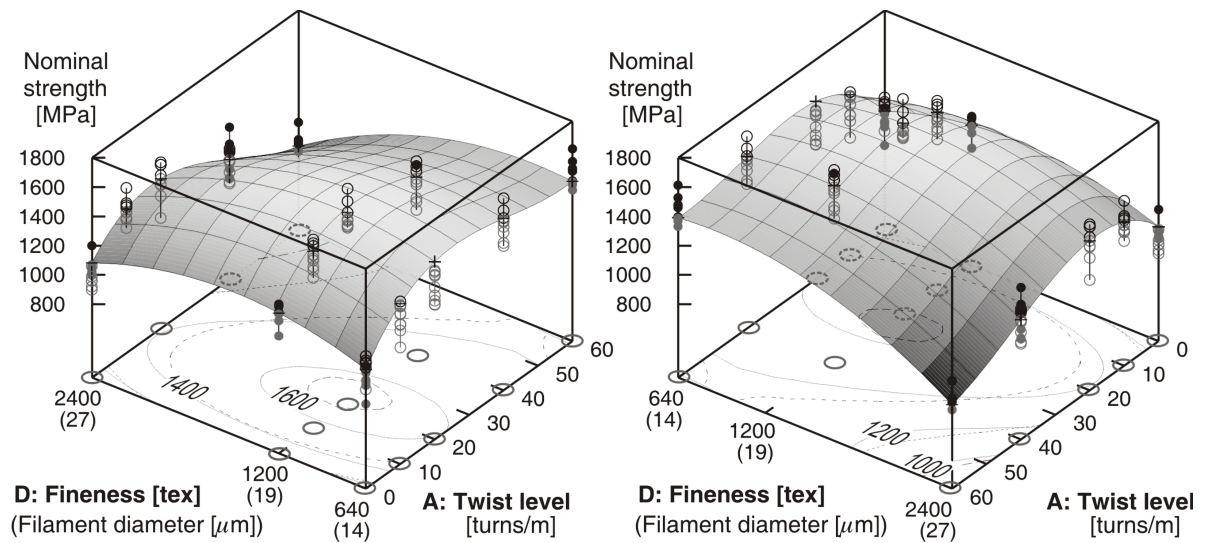


**Fig. 2:**  $\sigma_{\max}$  (Design I + II) depicted from two opposite viewpoints. For the combination: rate = 40 %/min and length = 500 mm. Empty circles: points belonging to design II. Continuous isolines: design I (compare with new dashed isolines for design I+II). Black and grey data points are above and below the surface, respectively.

The strength response surface resulting from the merged design I+II is shown from two viewpoints in Figure 2. The figure contains the almost identical surfaces both for design I and design I + II. The surfaces do not differ in the structure of the approximation but differ slightly in the regression coefficients. Their difference is indicated by the isolines in the **A-D** plane. Apparently, the inclusion of the new data in the approximation did not change the response surface significantly so that it can be concluded that design II confirmed the trends and the champion specimen was identified for the combination (**A** = 20 turns/m, **D** = 1200 tex).

### 4.3 Interpretation of the response

Two main questions are to be addressed in the phenomenological interpretation of the results: what are the reasons for the continuous strength increase in the range 0-20 turns/m and for its reduction at higher twist levels. These aspects can be discussed with the help of the stress-strain diagrams shown in Figure 3 in two different views. While the first row allows the reader to qualitatively compare the shapes of stress-strain diagrams for the pairs of twist 0 and 20 (left) and 0 and 60 (right) turns/m, the second row completes the picture by showing the full set of measured curves for 20 and 60 turns/m.

Comparing the stress-strain diagrams for the twist levels **A** = 0 and 20 in Figure 3 left, we observe that for the non-twisted reference yarns, there is a higher amount of slack (delayed activation) than for **A** = 20 turns/m. This means that raw yarns have production-induced



waviness and that the differences in the filament length due to this waviness get reduced at moderate levels of twist.

The second feature of the stress-strain diagram to note is that for non-twisted yarns filament breakages are spread over a wide range of nominal strain. This indicates independent failure of filaments in conjunction with a high scatter in filament breaking strain. Visually, the specimens failed with filaments randomly breaking along the yarn without localization at some cross section. The random distribution of breaks along the yarn leads to a high internal friction in the post-peak range.

Third, in contrast to the non-twisted yarns, the twist level 20 turns/m leads to a simultaneous failure of all filaments at significantly higher stresses followed by a sudden localized failure. The only explanation for this increase is a strong interaction between the filaments (local load sharing). In our opinion, the mentioned reduction of waviness due to improved filament packing cannot sufficiently explain the homogeneous behavior of the bundle. The amount of scatter in breaking strain did not vanish for the twisted yarns. Therefore, the filament breakages at the high stress level must have been compensated by the inter-filament bonding. Such scenario would correspond to the fragmentation discussed by Pan et al. [11]. This issue shall be clarified in the future both experimentally and using numerical models.

In Figure 3 top-right, the opposite tendency in strength evolution is shown on the example of the twist levels 20 and 60. The amount of slack gets very large for twist level 60 indicating high irregularity in the yarn packing leading to an increased structural influence of twist. On the other hand, these specimens exhibit also a sudden failure (Figure 3 right) indicating a high amount of interaction. In view of the studies presented in [4] for zero-twist this is unexpected since the spread in filament activation should lead to the spread in the filament failure on the first-come-first-go basis. The discrepancy could be explained by irregular packing of filaments due to over-twisting the yarn into compact and loose segments along and across the yarn (comp. Figure 1 right). While the loose segments explain the slow filament activation, the compact segments cause the brittle localized failure. This behavior might correspond to the wrapped ribbon packing described in [9].

Another important characteristic of the test response is the maximum achieved yarn (structural) stiffness  $E_{\max}$ . It can be used to assess the maximum amount of simultaneously activated filaments during the loading history. The results indicate that for moderate twist levels the maximum material stiffness approaches the  $E$ -modulus of glass (70 GPa) meaning that for some nominal strain all filaments contributed to the stress transfer. For maximum twist level, the amount of activated filaments gets significantly reduced. The fineness influences the material stiffness in the range (68 - 72 GPa) as a weak quadratic main effect. Further details concerning the measured stiffness and are provided in [19].

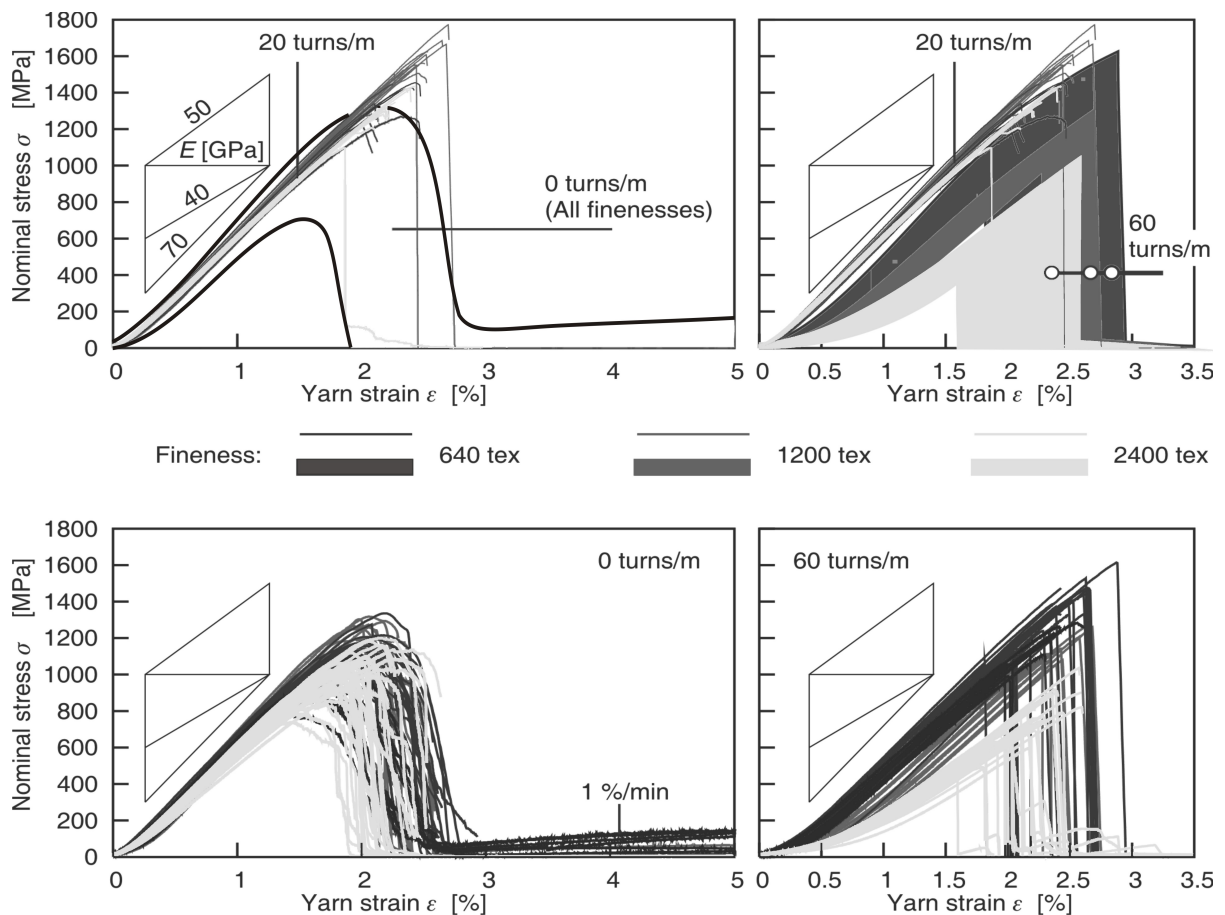


**Fig. 3:** Stress-strain diagrams. Top row: 20 turns/m compared to envelopes of zero twist level (left, all finenesses) and 60 turns/m (right, distinguished finenesses). Bottom row: detailed view on zero twist level (left) and 60 turns/m (right).

## 5 Conclusions

The multivariate study of continuous AR-glass multifilament yarns brought about an evidence of interaction between filaments through increase of bundle strength for a certain range of bundle twist. In particular, the study has identified a significant effect of bond on the yarn performance for twist levels up to 20 turns/m. The increased filament-filament interaction can compensate for filament breaks during the loading and results in significantly higher bundle strength. We attribute this increase to the fragmentation of filaments in agreement with the description in [11]. However, as mentioned in the beginning, the strain homogenization along the filaments could also induce strength increase [9].

As mentioned, the study was performed in the context of the research on textile-reinforced concrete exhibiting partial penetration of the yarn cross section. It should be emphasized that an improved performance of twisted yarns in tensile test cannot be reproduced in the

composite. The reason for this is that twisting hinders the penetration of the matrix into the yarn with the consequence of lower outer bond. However, this was not the intention behind the present study. The twisting has been imposed in order to study the bond between filaments and its interaction with lateral forces. These definitely occur in the composite for example in the vicinity of bridged cracks.

## 6 Acknowledgments

The work has been supported by German Science Foundation under project numbers GR1311/13-1 and CH276/1-1. Additionally, the work of the second author has also been supported by The Ministry of Education, Youth and Sports of the Czech Republic under project no. 1M06005 (Civak) and partially also by the Czech Science foundation under doctoral project GD103/09/H085. This support is gratefully acknowledged.

## References

- [1] SWAMY, R.; HUSSIN, M.: Continuous woven polypropylene mat reinforced cement composites for applications in building construction. In: HAMELIN P, VERCHERY G (eds.): *Textile Composites in Building Construction*, Paris: Pluralis, 1990, Part 1. pp. 55–67.
- [2] MEYER, C.; VILKNER, G.: Glass Concrete Thin Sheets Prestressed with Aramid Fiber Mesh. In: Naaman AE, W H, Arbor RA (eds.): *Fourth International RILEM Workshop on High Performance Fiber Reinforced Cement Composites (HPFRCC4)*, 2003, Bagnoux : RILEM Publications SARL, 2003, pp. 325–336.
- [3] PELED, A.; BENTUR, A.: Geometrical characteristics and efficiency of textile fabrics for reinforcing composites. *Cement and Concrete Research*. 2000; 30(5), pp. 781–790.
- [4] CHUDOBA, R.; VOŘECHOVSKÝ, M.; KONRAD, M.: Stochastic modeling of multi-filament yarns I: Random properties within the cross section and size effect. *International Journal of Solids and Structures* 43(3-4) (2006), pp. 413–434.
- [5] VOŘECHOVSKÝ, M.; CHUDOBA, R.: Stochastic modeling of multi-filament yarns: II. Random properties over the length and size effect. *International Journal of Solids and Structures* 43(3-4) (2006), pp. 435–458.
- [6] HEGGER, J.; WILL, N.; BRUCKERMANN, O.: Load-bearing behavior and simulation of textile reinforced concrete. *Materials and Structures* 39(8) (2006), pp. 765–775.
- [7] ZHOU, Y.; JIANG, D.; XIA, Y.: Tensile mechanical behavior of T300 and M40J fiber bundles at different strain rate. *Journal of Materials Science* 36(4) (2001), pp. 919–922.

- 
- [8] PHOENIX, S.L.; TAYLOR, H.M.: The asymptotic strength distribution of a general fiber bundle. *Advances in Applied Probability* 5 (1973), pp. 200–216.
- [9] HEARLE, J.W.S.; GROSBERG, P.; BACKER, S.: Structural mechanics of fibers, yarns, and fabrics. New York, London, Sydney, Toronto : Wiley-Interscience; 1969.
- [10] PHOENIX, S.L.: Statistical Theory for the Strength of Twisted Fiber Bundles with Applications to Yarns and Cables. *Textile Research Journal* 49 (1979), pp. 407–423.
- [11] PAN, N.; HUA, T.; QIU, Y.: Relationship between fiber and yarn strength. *Textile Research Journal* 71(11) (2001), pp. 960–964.
- [12] BROUGHTON, R.M.; MOGAHZY, Y.E.; HALL, D.M.: Mechanism of yarn failure. *Textile Research Journal* 92(3) (1992), pp. 131–134.
- [13] REALFF, M.L.; PAN, N.; SEO, M.; BOYCE, C. M. ET AL.: A stochastic simulation of the failure process and ultimate strength of blended continuous yarns. *Textile Research Journal* 70(5) (2000), pp. 415–430.
- [14] JONES, J.E.; HADDAD, G.N.; SUTTON, J.E.: Tensile Characteristics of Twisted Continuous-Filament Glass Yarns. *Textile Research Journal* 41(11) (1971), pp. 900–904.
- [15] MONTGOMERY, D.C.: *Design and Analysis of Experiments*. 5<sup>th</sup> Ed., Hoboken, USA : John Wiley & Sons Inc, 2001, 644 p.
- [16] DEAN, A.; VOSS, D.: *Design and Analysis of Experiments*. NY : Springer, 1999, 736 p.
- [17] HADDAD, G.N.; SUTTON, J.E.: Application of the Law of Composites to Twisted Continuous-Filament Glass/Nylon Blended Yarns. *Textile Research Journal* 42(8) (1972), pp. 452–459.
- [18] RAO, Y.; FARRIS, R.J.: A modeling and experimental study of the influence of twist on the mechanical properties of high-performance fiber yarns. *Journal of applied polymer science* 77(9) (2000), pp. 1938–1949.
- [19] CHUDOBA, R.; VOŘECHOVSKÝ, M.; ECKERS, V.; GRIES, T.: Effect of Twist, Fineness, Loading Rate and Length on Tensile Behavior of Multifilament Yarns (A Multivariate Study). *Textile Research Journal* 77(11) (2007), pp. 880–891.